

Ternary Emission of Fluorescence and Dual Phosphorescence at Room Temperature: A Single-Molecule White Light Emitter Based on Pure Organic Aza-Aromatic Material

Changjiang Zhou, Shitong Zhang, Yu Gao, Haichao Liu, Tong Shan, Xiaoming Liang, Bing Yang,* and Yuguang Ma

Herein, a simple aza-aromatic compound dibenzo[a,c]phenazine (DPPZ), which exhibits single-molecule white light with a ternary emission, consisting of simultaneous fluorescence ($S_1 \rightarrow S_0$) and dual room-temperature phosphorescence (RTP, $T_2 \rightarrow S_0$ and $T_1 \rightarrow S_0$) is reported. The Commission Internationale de l'Éclairage coordinates of DPPZ powder are (0.28, 0.33). To everyone's knowledge, this is the first case to achieve single-molecule white emission with ternary emission of fluorescence and dual RTP. This finding provides a prototype strategy to realize low-cost, stable pure organic single-molecule white light emission with three standard primary colors through further precise modulation of excited states.

white-light emission, such as phase separation, color-aging, fabrication complexity, etc.^[3] As a comparison, a single emitter with dual emission or multiemission could be a more promising alternative to realize organic white-light emission by solving the problems above. Without exception, more and more dual emission organic materials have been reported with single-molecule white light emission (SMWLE). In principle, dual emission can be assigned to two emissive sources of excited state: the lowest singlet (S_1) excited state for blue fluorescence and another excited state for a largely redshifted emis-

1. Introduction

Organic white-light materials are closely related to our daily life, due to its wide applications in lighting and display systems.^[1] In chroma theory, the white-light emission can be mainly obtained by two ways: one is the mixture of two complementary colors (yellow and blue), and the other is the most widely used complex of three primary colors (red, green, and blue).^[2] Therefore, multicomponent emitters with different emission colors are usually required to combine white-light emission. However, there are still many defects for the multiemitter


sion, including charge-transfer (CT) state,^[4] excimer state,^[5] proton-transfer state,^[6] the lowest triplet (T_1) excited state emission for room-temperature phosphorescence (RTP),^[7] etc. What's more, the latest SMWLE has been discovered with dual RTP emission by Tang's group.^[8] However, in principle, three-primary-color system is more convenient for regulating purer white emission, nevertheless, SMWLE with multiemission (at least ternary emission) has never been reported so far, let alone its structure–property relationship.

The development of single-molecule white light material consisted of pure organic RTP is very challenging for the following reasons. On one hand, in pure organic materials, the spin–orbit coupling (SOC) is always too small to afford the efficient intersystem crossing (ISC) for triplet exciton generation. On the other hand, the nonradiative process, including vibrational relaxation, ISC, and exogenous quenching, would further aggravate the waste of triplet excitons due to the long lifetime.^[9] Accordingly, in order to achieve efficient RTP in pure organic materials, two key countermeasures should be adopted: one is to accelerate ISC process for adequate triplet exciton generation; the other is to suppress nonradiative deactivation of triplet excitons, but the former is more important. According to the Fermi's Golden rule,^[10] the efficient radiation of triplet excitons mostly depend on an adequate accumulation of triplet excitons, acquiring for the enhancement of SOC to accelerate the ISC process. In pure organic material system, one way to realize large SOC is to introduce heavy atom such as halogen (such as Br and I) and deuterium.^[11] However, heavy halogen substitution seriously affects the chemical stability upon thermal and electrical treatments, and deuterium substitution is still of large expenses.

C. Zhou, Dr. S. Zhang, Dr. Y. Gao, Dr. H. Liu, T. Shan, Prof. B. Yang
State Key Laboratory of Supramolecular Structure and Materials
Jilin University
Changchun 130012, P. R. China
E-mail: yangbing@jlu.edu.cn

C. Zhou, Dr. S. Zhang, Dr. Y. Gao, Dr. H. Liu, T. Shan, Prof. B. Yang
College of Chemistry
Jilin University
Changchun 130012, P. R. China
Dr. S. Zhang
Institute of Theoretical Chemistry
Jilin University
Changchun 130012, P. R. China

X. Liang, Prof. Y. Ma
State Key Laboratory of Luminescent Materials and Devices
South China University of Technology
Guangzhou 510640, P. R. China

 The ORCID identification number(s) for the author(s) of this article can be found under <https://doi.org/10.1002/adfm.201802407>.

DOI: 10.1002/adfm.201802407

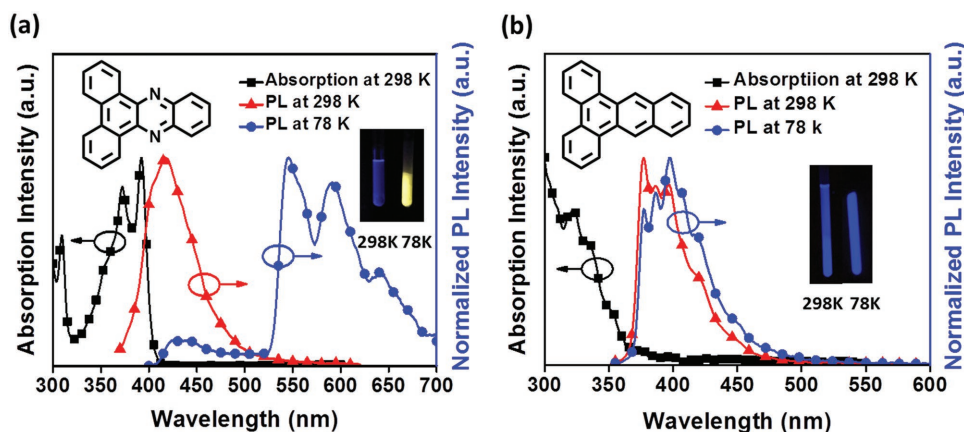


Figure 1. The chemical structure, absorption and emission spectra of a) DPPZ and b) DPAN in THF solution under 298 and 78 K. The insets are the photos of the steady-state emission of DPPZ and DPAN, respectively. The excitation wavelength for DPPZ and DPAN are 390 and 330 nm, respectively.

In principle, some light heteroatoms can also play a similar role as that of heavy atoms, which provide the lone pair electrons to strengthen SOC and to facilitate ISC process between $n \rightarrow \pi^*$ and $\pi \rightarrow \pi^*$ character states according to the El-Sayed rule,^[12] for instance, involving boron atom or carbonyl substitution in pure organic system.^[13] Furthermore, the other heteroatoms need to be systematically examined for the expansion of pure organic RTP material family. In this contribution, a SMWLE is harvested with the mixing three emissions of fluorescence and dual RTP of a nitrogen (N)-containing heterocyclic aromatic compound dibenzo[a,c]phenazine (DPPZ), as shown in **Figure 1**. Experimental and theoretical investigations reveal that the dual RTP is composed of a normal T_1 phosphorescence and an unusual T_2 phosphorescence from high-lying triplet state (exception to Kasha's rule). More importantly, the two RTP components of DPPZ are proved to be relatively independent, which creates a possibility of the rational excited state regulation for the desired SMWLE materials with standard tricolor. Our results not only provide a new concept for designing pure organic SMWLE material, but also propose a prototype strategy to design a single-molecule true white-light emitter with three standard primary colors in the future.

2. Results and Discussions

2.1. Photophysical Properties

2.1.1. Dispersed Condition

DPPZ is facilely synthesized using a one-step cyclization reaction with a high yield (Supporting Information). First, the absorption and emission spectra of DPPZ are recorded at different temperature in tetrahydrofuran (THF) for its S_1 and T_1 energy levels. As shown in **Figure 1**, DPPZ demonstrates a structured absorption, while its photoluminescence (PL) spectrum is structureless arising from the $n \rightarrow \pi^*$ transition character induced by nitrogen heteroatom. Due to the rigidity of planar structure, DPPZ shows very small Stokes shift between absorption and emission at room temperature (298 K). For the purpose of comparison, both absorption and emission are also

measured for a nitrogen-free counterpart DPAN in **Figure 1b**. As a matter of course, DPAN shows structured PL spectrum, corresponding to a $\pi \rightarrow \pi^*$ transition character.

In usual cases, the fluorescence of an organic emitter will hide the weak phosphorescence in its PL spectrum, since the radiative transition rate of phosphorescence is three or four orders of magnitude lower than that of fluorescence in pure organic materials. Therefore, to detect the phosphorescent emission, low-temperature circumstance is often adopted to suppress the nonradiation decay, and time-resolved measurements are always further adapted to exclude the interference of fluorescence signals. However, in DPPZ solution, we are surprised to find out that the steady-state PL is dominated by a structured $\pi \rightarrow \pi^*$ phosphorescence with a long lifetime of 2.7 μ s (**Figure S1**, **Table S1**, Supporting Information), and the fluorescence is only a residue at low temperature (78 K). This unusual phenomenon can be initially understood by the El-Sayed rule that ISC process takes places more easily, as a result of the distinct transition pattern between singlet and triplet states. In the case of DPPZ, the fluorescence is of structureless $n \rightarrow \pi^*$ transition character while its phosphorescence is assigned to $\pi \rightarrow \pi^*$ transition (refer to **Figure 4a**), which efficiently facilitates ISC process that contributes to the adequate triplet exciton generation for such significant steady-state phosphorescence. An evidence to well support this point is that the phosphorescence of DPAN cannot be observed under the same condition, indicating that N-heteroatom of DPPZ plays the key role in efficient triplet exciton generation, which is a crucial structure basis for RTP property. Notably, compared with DPAN (8.66 ns), the fluorescence lifetime of DPPZ is very short (0.072 ns, reported by Tian's group)^[14] and it could not even be resolved with a picosecond laser (**Figure S3**, Supporting Information), indicating that very fast ISC process is expected to occur from S_1 excited state in DPPZ.

Similar to the low-temperature, nonradiative transition can also be alleviated or suppressed to certain extent by rigid surrounding medium and intermolecular aggregation. Typically, a large number of molecules have been observed with enhanced PL emission upon the increase of viscosity or aggregation degree, knowing as the famous aggregation-induced emission (AIE) phenomenon, such as silole and tetraphenylethylene

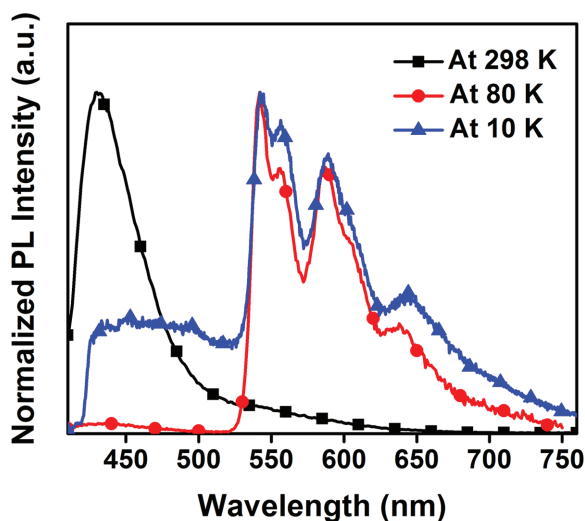


Figure 2. The PL spectra of DPPZ-doped film in PMMA at different temperatures. The excitation wavelength is chosen as 390 nm.

derivates.^[15] Likewise, the concept of AIE can also apply to the RTP, such as doping in rigid matrix (e.g., polymethyl-methacrylate, PMMA), crystallization, etc. In fact, for DPPZ, PMMA doping could be some effective access to RTP. In **Figure 2**, relative to that in THF solution, the DPPZ doped film (5% w/w in PMMA) demonstrates an extra tailing peak from 500 to 650 nm, which can be assigned to phosphorescence emission. As for the reason, the PL decay at 546 nm is fit with a long lifetime of 20.11 μ s, which is obviously distinguished from the short one as 0.3 ns of DPPZ fluorescence at 428 nm. Moreover, this RTP could also be confirmed by time-resolved PL measurement. With a delay time of 50 μ s, an obvious phosphorescent emission can be observed with vibrational fine structure between 541 and 586 nm, while the fluorescence emission fades to an inconspicuous residue, which is similar to that of THF solution at 78 K.

However, it seems to be impossible that we could still observe the “fluorescence component” of DPPZ with a long delay time of 50 μ s (Figure S5, Supporting Information), since the lifetime of the fluorescence component has been proved to be very short. Therefore, the fluorescence-like residue should originate from other emissive species. Considering that low temperature could restrict the nonradiative processes, we further carry out temperature-dependent experiment to clarify the origin of this fluorescence-like residue. Under a set of decreasing temperatures from 320 to 80 K, the phosphorescence of DPPZ-doped film gradually enhances (Figure S6, Supporting Information), with almost no change on the spectral shape. When the temperature is further lowered to 10 K, not only the fluorescence exhibits an enhancement due to the further suppressed nonradiation of S_1 excited state, but also an obvious new emission band emerges from 460 to 520 nm between fluorescence at 424 nm and phosphorescence at 541 nm (Figure 2), corresponding to the residue emission peak. According to the Kasha’s rule,^[16] the emission of an organic molecule should result from the lowest singlet (S_1) or triplet (T_1) excited state in general, nevertheless, both S_1 and T_1 emissions do coexist with the new emission band at 10 K. As a result, the new emission band at 10 K should

be ascribed to the emission from high-lying triplet T_n excited state as an exception to Kasha’s rule rather than a high-lying singlet S_n emission, since the peak of the new emission band is redshifted relative to the S_1 emission.

2.1.2. Single-Molecule White Light Emission in Aggregated Condition

Interestingly, the mixed emissions of S_1 , T_1 , and T_n are observed even more clearly in the neat powder of DPPZ, especially for T_1 and T_n mixed RTP, as shown in **Figure 3a**. Thus, the powder of DPPZ exhibits pure, stable white-light emission with a Commission Internationale de L’Eclairage (CIE) coordinate of (0.28, 0.33), with a photoluminescence quantum yield (PLQY) of 1%, as a result of the good continuity of PL spectrum that covers the whole visible region from 400 to 700 nm. Importantly, this simultaneous ternary emission may provide a prototype of SMWLE with standard three-primary-color mixing mechanism. Furthermore, these three different emissive components (fluorescence and dual phosphorescence) can be confirmed by the time-resolved PL spectra (Figure 3b). At a delay time of 160 μ s, the fluorescence component of DPPZ disappears completely, and only dual phosphorescence (T_n and T_1) remained obviously. What’s more, relative to T_1 phosphorescence, the T_n emission band from 480 to 530 nm demonstrates a synchronous and faster decay in a timescale of 1.4 ms, assigning to a vibronic splitting of RTP from high-lying T_n excited state in DPPZ, which could also be revealed by further peak fitting of the PL spectra of DPPZ (Figure 3a). Another solid evidence for the existence of T_n emission is the PL grinding effect and oxygen quenching effect in DPPZ neat powder (Figure S9, Supporting Information). In fact, according to the typical AIE experiment on DPPZ (PL spectra in the mixed solvent of water and tetrahydrofuran, Figure S10, Supporting Information), we found that RTP of DPPZ largely depends on its aggregation degree.^[17] Although tentatively we could not obtain high-quality crystal of DPPZ for molecular aggregation details, the powder X-ray diffraction (pXRD) reveals a partially crystalline state in DPPZ neat powder. After thoroughly grinding, the crystalline structure of DPPZ is fully destructed, and both T_1 and T_n RTP emissions exhibit more serious quenching comparing to that of fluorescence and shows more obvious sensitivity to the oxygen quenching, indicating that the phosphorescence is more dependent on the aggregation degree of DPPZ, which is essentially consistent with their phosphorescence instinct.

More importantly, the two RTP components of DPPZ are relatively independent to each other, which is beneficial to the emission stability that could guarantee the continuous white PL of DPPZ. In Figure 3c, instead of the T_n -RTP, the T_1 -RTP of DPPZ shows obvious enhancement upon the increasing of temperature, which not only implies that the $S_1 \rightarrow T_1$ ISC process is very efficient in DPPZ, but also reveals that the $T_1 \rightarrow T_n$ thermally activated reversed inner conversion mechanism^[8,18] is invalid in DPPZ, otherwise an enhancement on the PL of T_n -RTP should be observed. As a result of the independency of its RTP components, DPPZ demonstrates obvious excitation wavelength dependency, revealing the different exciton resources of three emissive species. In Figure 3d,

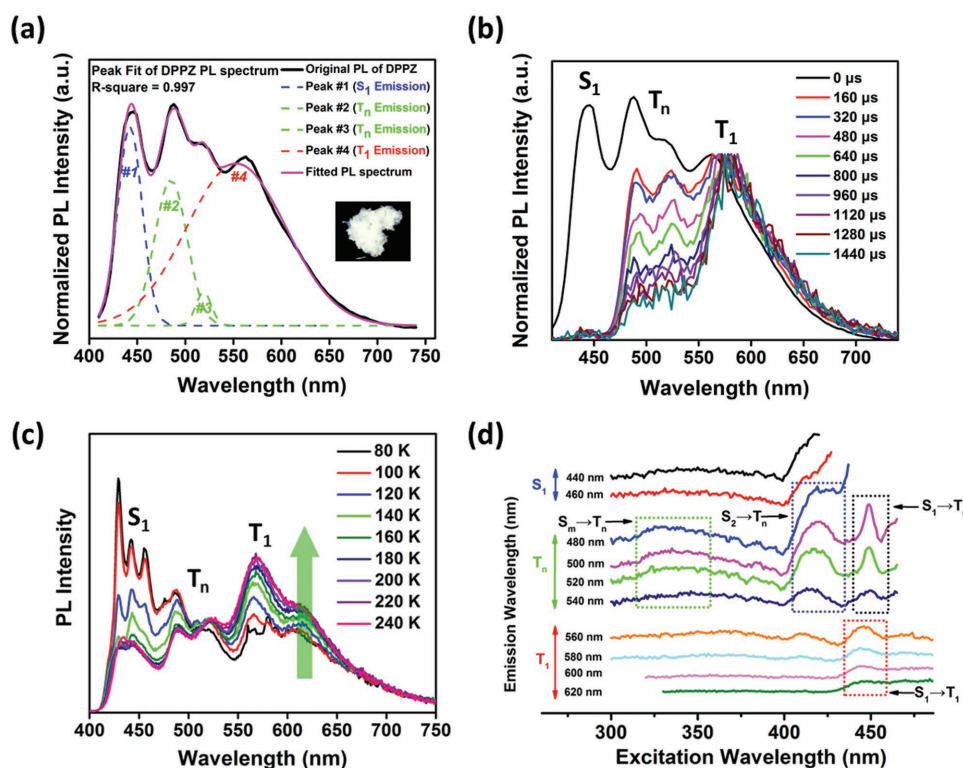


Figure 3. The RTP properties of DPPZ neat powder. a) PL spectrum and peak fitting of DPPZ neat powder under ambient conditions. b) Normalized time-resolved PL spectra of DPPZ neat powder. The spectra are normalized to the T_1 emission for comparison. c) Temperature-dependent PL spectra from 80 to 240 K. d) Excitation spectra of DPPZ at different emission wavelengths (440–620 nm). The spectra of (a) and (b) are given as normalized ones to guarantee that the results are comparable relative strengths.

the obvious excitation of T_1 -RTP only appears at ≈ 445 nm with negligible contribution from higher excitations, corresponding to the ISC channel of $S_1 \rightarrow T_1$. As a comparison, the excitations of T_n -RTP (emission wavelengths from 480 to 540 nm) demonstrate three series of markedly bands at ≈ 330 , ≈ 420 , and ≈ 445 nm, respectively, indicating that T_n -RTP could be efficiently generated through multiple alternative ISC channels. In this regard, it is convincing that T_1 -RTP and T_n -RTP have totally different origins. For T_n -RTP, two main ISC channels can be probably assigned to $S_1 \rightarrow T_2$ and $S_2 \rightarrow T_2$ upon the excitations at ≈ 420 and ≈ 445 nm, respectively. Additionally, it should be mentioned that the influence of triplet absorption can be excluded here, since the triplet absorption of DPPZ has been confirmed to be very weak and of even lower energy level (≈ 550 nm).^[14]

2.2. Theoretical Analysis of the Single-Molecule White Light Emission

To further clarify the essence of the dual RTP in DPPZ, time-dependent density functional theory (TDDFT) calculations are carried out.^[19] First, the T_n -RTP species of DPPZ could be specified as a T_2 -RTP emission. To confirm this point, we calculated the natural transition orbital (NTO) of relevant excited states to understand their transition characters, as shown in Figure 4a. On one hand, the “hole” of S_1 and T_2 excited states do not possess any nodal section along molecular plane, assigning to σ -bonding character between any two atoms. For

the two sp^2 -N heteroatoms, a p-orbital character of lone pair electron was obviously observed, indicating n-electron character of “hole” wavefunction. On the other hand, the “particles” possess such nodal section along molecular plane, and are all delocalized over the whole molecular skeleton, which are of obvious π -bonding character. Thus, both S_1 and T_2 excited states of DPPZ should be attributed to $n \rightarrow \pi^*$ transition. As a contrast, both S_2 and T_1 excited states should be assigned to $\pi \rightarrow \pi^*$ transition.^[20] According to the El-Sayed rule, the ISC processes along $S_1 \rightarrow T_1$ and $S_2 \rightarrow T_2$ are expected to occur efficiently in DPPZ (Figure 4a) due to the different transition patterns, which are in good agreement with the excitation-wavelength-dependent results. Second, the SOC for $S_1 \rightarrow T_1$ and $S_2 \rightarrow T_2$ are estimated by Beijing Density Function (BDF) program^[21] as 10.33 and 6.03 cm^{-1} , respectively, which can well rationalize the efficient ISC processes of $S_1 \rightarrow T_1$ and $S_2 \rightarrow T_2$, especially for the generation and accumulation of T_2 excitons. The last but not the least, the existence of T_2 -RTP reveals that DPPZ does not only benefit from adequate exciton resources, a fast radiative rate of T_2 excited state is also needed. The radiation rate constants of T_2 and T_1 excited states are calculated to be 4.00×10^5 and $1.82 \times 10^5 \text{ s}^{-1}$, respectively,^[22] which is in correspondence of their characterful lifetimes (13.33 and 24.68 μ s, respectively, Table S1, Supporting Information).

Additionally, due to the different transition patterns between T_2 and T_1 , the internal conversion (IC) of $T_2 \rightarrow T_1$ should be probably slowed down to some extent.^[23] Meanwhile, the $n \rightarrow \pi^*$ transition character of T_2 unblocks the radiative transition of

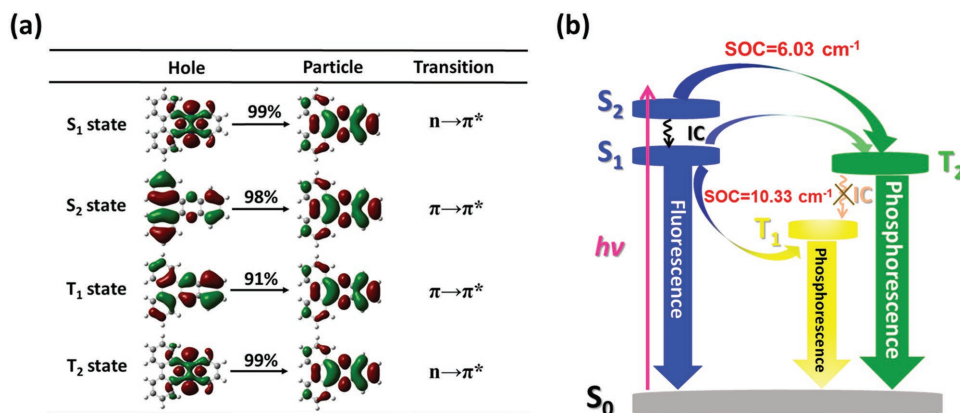


Figure 4. a) Natural transition orbitals (NTO) images of the S₁, S₂, T₁, and T₂ excited states of DPPZ. The NTO images of each excited states represent for their transition forms from the “hole” unity to the “particle” unity, respectively, and the percentages on the arrows are the proportions of the transitions. b) Schematic Jablonski diagram with SOC matrix elements of RTP-related ISC processes in DPPZ.

T₂→S₀.^[8] Thus, the radiative transition of T₂→S₀ can compete with the limited IC process of T₂→T₁, and finally leading to the dual phosphorescent emission of a T₂→S₀ RTP with a short lifetime and a T₁→S₀ RTP with a little long lifetime, which is consistent with the excitation-wavelength-dependent results. Finally, besides ISC channels of S₂→T₂ and S₁→T₁, the S₁→T₂ channel is also active. Although the SOC of S₁→T₂ is relatively small (0.23 cm⁻¹), the calculated energy gap between them is very small ($E_{S_1} - E_{T_1} = 0.14$ eV, Figure S15, Supporting Information), which is identical to the excitation band of T₂-RTP around 440 nm in Figure 3d. As a comparison, the large SOC is not found in the nitrogen-free counterpart DPAN, indicating that nitrogen heteroatom surely plays a crucial role in the RTP of DPPZ, and it is an important molecular design prototype to achieve simultaneous multiemission based on single molecule.

3. Conclusion

To sum up, we synthesized a pure-organic aromatic compound dibenzo[a,c]phenazine (DPPZ), and successfully achieved a pure organic single-molecule white-light emission at ambient condition. The CIE coordinate of DPPZ emission is (0.28, 0.33), as a result of the continuous PL emission covering the whole visible region from ternary emissions: S₁-fluorescence, T₁-RTP, and T₂-RTP (exception to Kasha's rule). Theoretical calculation combined with photophysical property characterization proves that T₁-RTP and T₂-RTP have relatively independent origin, which is beneficial for the continuity and stability of the white emission of DPPZ. The aromatic system containing nitrogen heteroatom turns out to be a promising candidate to enhance SOC, leading to the efficient ISC in pure organic metal-free RTP materials, instead of commonly used heavy atoms (e.g., bromine, iodine, or deuterium) and carbonyl group. Our results not only provide a new molecular system to develop environmental-friendly, low-cost, stable pure organic SMWLE materials, but also suggest a prototype mechanism to realize single-molecule true white light emission with standard three-primary-color

mixing through a precise manipulation on the energy levels of three different excited states in the future.

4. Experimental Section

All the reagents and solvents used for the synthesis were purchased from Aldrich and Acros companies and used without further purification. The synthesis procedure was presented in Scheme S1 (Supporting Information). The ¹H NMR and ¹³C NMR spectra were recorded on AVANCE 500 spectrometers at 298 K by utilizing deuterated dimethyl sulfoxide (DMSO) and deuterated chloroform (CDCl₃) as solvents and tetramethylsilane (TMS) as a standard, respectively. The compounds were characterized by a Flash EA 1112, CHNS-O elemental analysis instrument. The matrix-assisted laser desorption/ionization time of flight mass spectrometry (MALDI-TOF-MS) mass spectra were recorded using an AXIMA-CFR plus instrument. Thermal gravimetric analysis (TGA) was undertaken on a PerkinElmer thermal analysis system at a heating rate of 10 °C min⁻¹ and a nitrogen flow rate of 80 mL min⁻¹. UV-vis absorption spectra were recorded on a UV-3100 spectrophotometer. PL spectra of original powder and ground powder in air, N₂, and O₂ were carried out with Edinburgh FLS-980. The time-resolved PL spectra of doped film were measured on a Horiba Fluoromax-4 spectrofluorometer. PL efficiency of powder was measured on quartz plate using an integrating sphere apparatus. The temperature-dependent spectra and lifetimes were measured on an Edinburgh FLS-980 with an EPL-375 optical laser. The time-resolved PL spectra of powder were measured on an Edinburgh LP-920. All the density functional theory (DFT) calculations and natural transitional orbital (NTO) analysis were carried out using Gaussian 09 (version D.01) package on a Power Leader cluster. The excited-state geometry was optimized by time-dependent density functional theory (TDDFT) with the B3LYP functional at the basis set level of 6-31G(d, p). The energy levels of singlet and triplet were obtained using TDDFT with the B3LYP functional at the basis set level of 6-31G(d, p) at the optimized excited state S₁ and T₁ geometries, respectively. The SOC matrix elements were calculated using a BDF package. The radiative rate constants were calculated using the Molecular Materials Property Prediction Package (MOMAP).

The synthesis of dibenzo[a,c]phenazine followed the procedure described in previous report.^[24] A mixture of phenanthrene-9,10-dione (1.04 g, 5 mmol) and benzene-1,2-diamine (0.54 g, 5 mmol) in acetic acid (80 mL) was heated to reflux for 8 h. After cooling to room temperature, the resulting mixture was poured into ethanol (200 mL), and then filtered. The solid was washed with ethanol several times. The crude product was purified by column chromatography on silica gel (eluent: dichloromethane) and dried under vacuum to give the desired

compound as a white solid in 80% yield (1.12 g). ^1H NMR (500 MHz, DMSO) δ 9.32 (d, J = 7.9 Hz, 2H), 8.84 (d, J = 8.1 Hz, 2H), 8.38 (dd, J = 6.4, 3.4 Hz, 2H), 8.02 (dd, J = 6.4, 3.3 Hz, 2H), 7.92 (t, J = 7.5 Hz, 2H), 7.85 (t, J = 7.5 Hz, 2H). ^{13}C NMR (126 MHz, CDCl_3) δ 142.60, 142.20, 132.01, 130.31, 129.68, 129.47, 127.94, 126.28, 122.92. MALDI-TOF MS (mass m/z): 280 $[\text{M}]^+$. Anal. calcd for $\text{C}_{20}\text{H}_{12}\text{N}_2$: C 85.69, H 4.31, N 9.99; found: C 85.95, H 4.21, N 9.92.

Supporting Information

Supporting Information is available from the Wiley Online Library or from the author.

Acknowledgements

C.Z. and S.Z. contributed equally to this work. This work was supported by the National Natural Science Foundation of China (51473063, 91233116, and 51673083), the National Key Basic Research and Development Program of China (Grant Nos. 2016YFB0401001, 2013CB834801, and 2015CB655003), the Postdoctoral Innovation Talent Support Project (BX201700097), and the China Postdoctoral Science Foundation (2017M620108).

Conflict of Interest

The authors declare no conflict of interest.

Keywords

high-lying triplet, room-temperature phosphorescence, spin–orbital coupling, ternary emission, white light

Received: April 9, 2018

Revised: May 15, 2018

Published online: June 21, 2018

- [1] a) K. T. Kamtekar, A. P. Monkman, M. R. Bryce, *Adv. Mater.* **2010**, 22, 572; b) M. Han, Y. Tian, Z. Yuan, L. Zhu, B. Ma, *Angew. Chem., Int. Ed.* **2014**, 53, 10908; c) M. Du, Y. Feng, D. Zhu, T. Peng, Y. Liu, Y. Wang, M. R. Bryce, *Adv. Mater.* **2016**, 28, 5963.
- [2] G. M. Farinola, R. Ragni, *Chem. Soc. Rev.* **2011**, 40, 3467.
- [3] a) Y. Liu, M. Nishiura, Y. Wang, Z. Hou, *J. Am. Chem. Soc.* **2006**, 128, 5592; b) S. H. Kim, S. Park, J. E. Kwon, S. Y. Park, *Adv. Funct. Mater.* **2011**, 21, 644.
- [4] H. Yan, D. Tu, P. Leong, S. Guo, C. Lu, Q. Zhao, *Angew. Chem., Int. Ed.* **2017**, 56, 11370.
- [5] Q. Y. Yang, J. M. Lehn, *Angew. Chem., Int. Ed.* **2014**, 53, 4572.
- [6] K.-C. Tang, M.-J. Chang, T.-Y. Lin, H.-A. Pan, T.-C. Fang, K.-Y. Chen, W.-Y. Hung, Y. H. Hsu, P.-T. Chou, *J. Am. Chem. Soc.* **2011**, 133, 17738.
- [7] a) Z. Mao, Z. Yang, Y. Mu, Y. Zhang, Y. F. Wang, Z. Chi, C. C. Lo, S. Liu, A. Lien, J. Xu, *Angew. Chem., Int. Ed.* **2015**, 54, 6270; b) S. Shao, J. Ding, L. Wang, X. Jing, F. Wang, *J. Am. Chem. Soc.* **2012**, 134, 20290.
- [8] Z. He, W. Zhao, J. W. Lam, Q. Peng, H. Ma, G. Liang, Z. Shuai, B. Z. Tang, *Nat. Commun.* **2017**, 8, 416.
- [9] a) G. Baryshnikov, B. Minaev, H. Agren, *Chem. Rev.* **2017**, 117, 6500; b) C. Sun, X. Ran, W. Huang, *J. Phys. Chem. Lett.* **2018**, 9, 335.
- [10] P. A. M. Dirac, *Proc. R. Soc. London, Ser. A* **1927**, 114, 243.
- [11] a) S. Hirata, K. Totani, T. Watanabe, H. Kaji, M. Vacha, *Chem. Phys. Lett.* **2014**, 591, 119; b) J. Xu, A. Takai, Y. Kobayashi, M. Takeuchi, *Chem. Commun.* **2013**, 49, 8447; c) O. Bolton, K. Lee, H.-J. Kim, K. Y. Lin, J. Kim, *Nat. Chem.* **2011**, 3, 205; d) D. Li, F. Lu, J. Wang, W. Hu, X.-M. Cao, X. Ma, H. Tian, *J. Am. Chem. Soc.* **2018**, 140, 1916.
- [12] a) M. El-Sayed, *J. Chem. Phys.* **1964**, 41, 2462; b) M. El-Sayed, *J. Chem. Phys.* **1963**, 38, 2834.
- [13] a) G. Zhang, G. M. Palmer, M. Dewhurst, C. L. Fraser, *Nat. Mater.* **2009**, 8, 747; b) X. Chen, C. Xu, T. Wang, C. Zhou, J. Du, Z. Wang, H. Xu, T. Xie, G. Bi, J. Jiang, *Angew. Chem., Int. Ed.* **2016**, 55, 9872; c) J. Yang, X. Zhen, B. Wang, X. Gao, Z. Ren, J. Wang, Y. Xie, J. Li, Q. Peng, K. Pu, *Nat. Commun.* **2018**, 9, 840.
- [14] J. Chen, Y. Chen, Y. Wu, X. Wang, Z. Yu, L. Xiao, Y. Liu, H. Tian, J. Yao, H. Fu, *New J. Chem.* **2017**, 41, 1864.
- [15] a) M. Wang, G. Zhang, D. Zhang, D. Zhu, B. Z. Tang, *J. Mater. Chem.* **2010**, 20, 1858; b) J. Luo, Z. Xie, J. W. Lam, L. Cheng, H. Chen, C. Qiu, H. S. Kwok, X. Zhan, Y. Liu, D. Zhu, *Chem. Commun.* **2001**, 1740.
- [16] M. Kasha, *Discuss. Faraday Soc.* **1950**, 9, 14.
- [17] a) S. S. Liow, H. Zhou, S. Sugiarto, S. Guo, M. L. S. Chalasani, N. K. Verma, J. Xu, X. J. Loh, *Biomacromolecules* **2017**, 18, 886; b) C. Y. Yu, H. Xu, S. Ji, R. T. Kwok, J. W. Lam, X. Li, S. Krishnan, D. Ding, B. Z. Tang, *Adv. Mater.* **2017**, 29, 1606167.
- [18] T. Itoh, *Chem. Rev.* **2012**, 112, 4541.
- [19] M. J. Frisch, G. W. Trucks, H. B. Schlegel, G. E. Scuseria, M. A. Robb, J. R. Cheeseman, G. Scalmani, V. Barone, B. Mennucci, G. A. Petersson, H. Nakatsuji, M. Caricato, X. Li, H. P. Hratchian, A. F. Izmaylov, J. Bloino, G. Zheng, J. L. Sonnenberg, M. Hada, M. Ehara, K. Toyota, R. Fukuda, J. Hasegawa, M. Ishida, T. Nakajima, Y. Honda, O. Kitao, H. Nakai, T. Vreven, J. A. Montgomery Jr., J. E. Peralta, F. Ogliaro, M. Bearpark, J. J. Heyd, E. Brothers, K. N. Kudin, V. N. Staroverov, T. Keith, R. Kobayashi, J. Normand, K. Raghavachari, A. Rendell, J. C. Burant, S. S. Iyengar, J. Tomasi, M. Cossi, N. Rega, J. M. Millam, M. Klene, J. E. Knox, J. B. Cross, V. Bakken, C. Adamo, J. Jaramillo, R. Gomperts, R. E. Stratmann, O. Yazyev, A. J. Austin, R. Cammi, C. Pomelli, J. W. Ochterski, R. L. Martin, K. Morokuma, V. G. Zakrzewski, G. A. Voth, P. Salvador, J. J. Dannenberg, S. Dapprich, A. D. Daniels, O. Farkas, J. B. Foresman, J. V. Ortiz, J. Cioslowski, D. J. Fox, Gaussian 09, Revision D.01, Gaussian, Inc., Wallingford, CT **2013**.
- [20] a) H. Ma, W. Shi, J. Ren, W. Li, Q. Peng, Z. Shuai, *J. Phys. Chem. Lett.* **2016**, 7, 2893; b) Z. Shuai, Q. Peng, *Phys. Rep.* **2014**, 537, 123; c) J. Yang, Z. Ren, Z. Xie, Y. Liu, C. Wang, Y. Xie, Q. Peng, B. Xu, W. Tian, F. Zhang, *Angew. Chem.* **2017**, 129, 898.
- [21] a) W. Liu, F. Wang, D. Dai, L. Li, M. Dolg, *Theor. Chem. Acc.* **1997**, 96, 75; b) W. Liu, G. Hong, L. Li, J. Theor. Comput. Chem. **2003**, 2, 257; c) K. Hirao, Y. Ishikawa, Vol. 5, *Recent Advances in Relativistic Molecular Theory*, World Scientific, Singapore **2004**, p. 257.
- [22] a) Q. Peng, Y. Yi, Z. Shuai, J. Shao, *J. Am. Chem. Soc.* **2007**, 129, 9333; b) Q. Peng, Y. Yi, Z. Shuai, J. Shao, *J. Chem. Phys.* **2007**, 126, 114302; c) Y. Niu, Q. Peng, Z. Shuai, *Sci. China, Ser. B: Chem.* **2008**, 51, 1153; d) Y. Niu, Q. Peng, C. Deng, X. Gao, Z. Shuai, *J. Phys. Chem. A* **2010**, 114, 7817; e) Q. Peng, Y. Niu, Q. Shi, X. Gao, Z. Shuai, *J. Theor. Comput. Chem.* **2013**, 9, 1132.
- [23] S. Wu, *Introduction of Polymer Photochemistry: Theory and Application*, Science Press, Beijing **2003**, p. 18.
- [24] S. Wang, X. Yan, Z. Cheng, H. Zhang, Y. Liu, Y. Wang, *Angew. Chem., Int. Ed.* **2015**, 54, 13068.